Semantic enrichment of urban space: A point cloud-based framework for road marking analysis

[1]Elisavet Tsiranidou, [1]Aiara Brea Portals, [1]Antonio Fernández Álvarez, [1]Lucía Díaz Vilariño

[1]CINTECX, Universidade de Vigo, GeoTECH group, 36310 Vigo, Spain (elisavet.tsiranidou, aiara.brea, antfdez, lucia)@uvigo.gal

Keywords: Point cloud processing, Traffic management, Intensity-based thresholding, Mobile laser scanning, Outdoor modelling

Abstract

In this paper, we present a method for the analysis of urban road markings using point cloud data, aiming to enhance the understanding and functionality of urban spaces. Our method employs intensity-based analysis along with hierarchical clustering and object descriptors to identify and categorize road markings while maintaining the original point cloud format. Then, we conceptualize a new space distribution from segmenting urban spaces into distinct functional areas based on road markings. Our results indicate the potential of our approach in providing insights that could support urban planning, and autonomous vehicle navigation systems, yet further research and validation are essential to fully realize its potential.

1. Introduction

Accurate interpretation of urban road environments is crucial for traffic management and autonomous vehicle navigation. Meghjani et al. (2019) presented a novel autonomous driving system that exploits road contextual information and the intentions of other road users for urban driving. Urban spaces are complex networks of movement and interaction between humans, vehicles, and the city itself, where streets are not just passageways, but platforms that serve as dynamic places where various interactions take place. Rasouli & Tsotsos, (2018) discussed the importance of communication in urban traffic to resolve ambiguity and examined the interaction between pedestrians and drivers (or vehicles) from the perspective of joint attention. Thus, urban road environment encompasses a deep understanding of the dynamic relationship between various elements that define urban mobility.

The delineation of space by road markings is a key aspect of the accurate interpretation of urban space. Diakité & Zlatanova, (2018) defined functional spaces as sub-areas with a designated purpose for carrying out specific tasks and interacting with objects relevant to the activity at hand. Delineating the outdoor, unbounded from above, functional spaces of urban environment is essential for providing more accurate identification of urban public spaces, thus specifying more precisely navigable areas. IndoorGML stands out as a prominent standard dedicated to the detailed modelling of indoor environments, providing a rich semantic and geometric framework adapted to the needs of indoor navigation. Conversely, CityGML, with its broad scope encompassing urban and landscape modelling, represents a less investigated aspect in the domain of urban space definition and characterization. Babić et al. (2020) conducted a systematic review of the influence of road markings on driver behaviour and overall road safety. The review highlights the critical role of road markings in guiding road users and their importance as a cost-effective safety measure.

Urban space distribution according to functionality can be defined from the road markings themselves. Their configuration is crucial for efficient traffic management and can significantly influence urban mobility patterns. Zebra crossings serve as safety features within the urban environment, providing designated pedestrian crossing points that prioritize pedestrian safety and encourage walkability. Their locations are carefully chosen to ensure visibility, connectivity, and accessibility, while promoting safe interactions between pedestrians and vehicles (Golakiya et al., 2019) examined the impact of mid-block pedestrian crossings on the speed characteristics and capacity of urban arterial road, highlighting the importance of designated crossing facilities such as zebra crossings for pedestrian safety and traffic efficiency.

Nowadays, remote-sensing techniques for urban information inventory are widely used due to their efficiency in collecting three-dimensional (3D) information of large areas. Generating urban networks has been studied in recent years mainly from the exploitation of aerial or satellite images. Although these types of data are widely available and allow the extraction of terrestrial objects such as roads, buildings, and even vegetation, they do not contain accurate geometry. On the other hand, point clouds enable us to extract precise locations and measurements of objects and provide accurate 3D geospatial information of roadways. Ma et al. (2018) provided a systematic review of existing literature related to the detection and extraction of urban objects using Mobile Laser Scanning (MLS) data. In their work, they highlighted the advantages and limitations of both 2D image-driven methods and 3D MLS point cloud methods.

In the last few years, the use of Mobile LiDAR point clouds has become an effective solution for providing three-dimensional highly accurate and dense data with rich geometric details of traffic objects. Therefore, they have been increasingly captured for the digitalization of the urban environment. Point cloud data provides a wealth of spatial information, and their effective processing and analysis can be used for accurately depicting and understanding complex urban roadways. This high-resolution, three-dimensional data offers detailed insights into the geometry of roads, the presence and condition of road markings, and the interaction between different urban elements.

This work focuses on the analysis of urban road markings from point clouds with the final aim of characterizing and distributing the urban space based on its functionality. The main contributions of this work are:

- A method for road marking detection from point clouds with intensity. No other attributes such as colour information or scan angle are used.
- A conceptual distribution of the road space and semantically enrichment from the road marking extraction.

This contribution has been peer-reviewed. The double-blind peer-review was conducted on the basis of the full paper.
https://doi.org/10.5194/isprs-annals-X-4-W5-2024-281-2024 | © Author(s) 2024. CC BY 4.0 License.

This paper is organized as follows: Section 2 provides a comprehensive review of point cloud processing methods for road marking extraction. Section 3 elaborates on the developed approach, while Section 4 shows the experiments and results obtained from applying the method to a real case study. Lastly, Section 5 is devoted to concluding this work.

2. Related work

Barçon et al. (2022) made a comprehensive review of the processing chains for road marking detection from dense MLS point clouds and underlined the contributions and limitations of existing methods. The authors suggest areas for further research and potential improvements in processing chains for road marking detection and classification. This might involve the development of more robust algorithms that can better handle the variability in data quality and environmental conditions, as well as leveraging advancements in machine learning and computer vision to improve detection accuracy. Also, by considering more contextual information about the surrounding environment and encoding spatial relationships between road objects. C. Ye et al. (2022) proposed a semi-automated method for extracting lane markings, especially on curved roads, from MLS point clouds. They utilized intensity thresholding and conditional Euclidean clustering algorithms for detecting textual and directional road markings. R. Yang et al. (2020) presented an accurate algorithm for detecting road markings from noisy point clouds generated by low-cost mobile LiDAR systems. This method effectively removes nonroad points and organizes the remaining points into pseudo-scan lines for road surface extraction and road marking detection, showing excellent performance. Certad et al. (2022) introduced a method to extract road markings from reflectivity data of a 64-layer LiDAR sensor. They employed plane segmentation, region growing clustering, and adaptive thresholding based on Otsu's method, demonstrating reliability and precision in road markings segmentation. Mi et al. (2021) proposed a two-stage coarse-to-fine approach for extracting and modeling road markings from MLS point clouds. This approach is robust to variations in reflective intensity, various point density, and partial occlusion, achieving high performance in extracting multiple types of road markings even with worn and incomplete markings. X. Y. Ye et al. (2020) presented a two-stage, real-time road marking detection framework based on the YOLOv2 architecture. The system is designed to address the challenges of road marking detection under varying environmental conditions such as illumination, weather, and angles of view. Y. Yang et al. (2020) proposed a method that improves point cloud simplification by using a modified fuzzy c-means (MFCM) clustering algorithm that preserves feature information. The algorithm combines gravitational search optimization with MFCM for efficient point cloud data division and simplification. Their novel clustering method based on spatial neighborhood connected region labeling, addresses the efficiency and resource consumption issues in large data processing. It accurately classifies datasets with a single parameter and effectively identifies both cluster and sparse outliers. In the research by (Wen et al., 2019) it is shown that deep learning can be applied to MLS data by converting the data into a 2D intensity image through rasterization. They suggest a modified Convolutional Neural Network (CNN) segmentation approach that considers both intensity and shape information to identify road markings. Initially, a multi-scale Euclidean clustering algorithm was employed to classify large-sized road markings, such as zebra crossings. Subsequently, the remaining small-sized road markings, including texts and diamonds, were classified into different groups using a four-layer convolutional network, followed by an optimized conditional generative adversarial network (c-GAN) to enhance the completeness of the extracted road markings. Hoang et al. (2019) focused on improving the accuracy of detecting and classifying road markings critical for autonomous vehicles. This research addresses the challenges associated with the detection and classification of arrows and bike markings on roads. Cheng et al. (2020) introduced an approach combining intensity thresholding and deep learning for extracting lane markings from LiDAR point clouds acquired by mobile mapping systems (MMS). The intensity thresholding strategy utilizes unsupervised intensity normalization to enhance the contrast between lane markings and the road surface, while the deep learning strategy employs a model trained on automatically labeled training data to accurately identify lane markings. Fang et al. (2022) introduced a graph attention network, named GAT SCNet, to categorize road markings into 11 different types using LiDAR point clouds. The GAT_SCNet model constructs sequential, computable subgraphs and utilizes a multi-head attention mechanism to incorporate the geometric and topological connections between nodes and their neighbors to compute various road marking descriptors.

Recent advances in urban object detection from point clouds have significantly enhanced urban space analysis, crucial for planning and navigation. Nikoohemat et al. (2019) introduced the Flexible Space Subdivision (FSS) framework, which automatically identifies navigable indoor spaces by classifying objects based on their mobility. Meanwhile, (González-Collazo et al., 2022) focused on defining functional spaces at bus stops using Mobile Laser Scanning (MLS) data, distinguishing areas for pedestrians, buses, and shared use. These studies contribute to a better understanding of urban dynamics by delineating spaces for specific functions and interactions.

3. Method

The method developed in this work starts from semantically segmented urban point clouds, as described in (González-Collazo et al., 2024) .The method relies on *road*, *sidewalk*, and *curb* classes, and the point cloud lacks colour information but contains LiDAR intensity attribute. Figure 1 shows a brief workflow summarizing the method.

3.1 Pre-processing

In the preliminary phase of this method, the road class is pre-processed to reduce its massive volume and address challenges caused by inconsistent distribution of intensity. These inconsistencies can arise due to a range of factors, such as material properties of the road, environmental conditions, or the angle of the scanning device. To ensure a uniform quality of data and to facilitate more accurate analysis, the point cloud is partitioned into several blocks or Regions of Interest (ROI). For this, the road centrelines of our data are utilized to delineate the Regions of Interest. The initial phase of this process involves dividing each centreline into uniform segments, keeping the edge points of them to define the boundaries of the ROIs. This consistent division between the segments ensures that the ROIs are of equal size. Then, the point cloud is loaded and segmented into cylindrical sections according to these edge points. However, we notice that on the curved roads, our initial method resulted in gaps between the segmented Regions of Interest. These gaps arise from the straight-line approximation applied to the inherently curved nature of the road's centreline, which does not accurately capture the road's geometry. To address this issue, we employ an algorithm that recalculates the midpoint of each segment by considering the curvature. This algorithm shifts the midpoint along the axis of the curve's arc, ensuring that the cylindrical

ROIs are correctly aligned with the curved centreline, thereby eliminating the gaps observed in the initial segmentation.

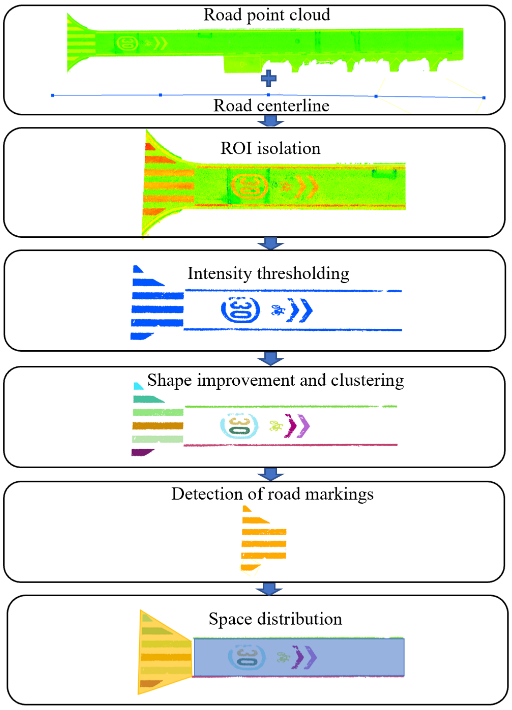

Figure 1. Workflow of the method.

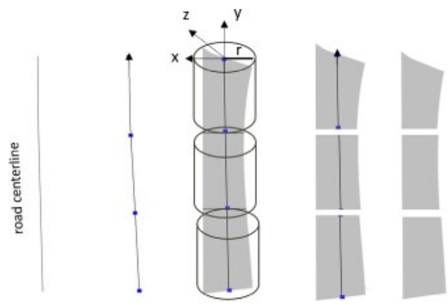

Figure 2. ROI generation through cylindrical sections.

3.2 Intensity analysis

Every method discussed in the literature leverages the significant difference in radiometric properties between road markings and road asphalt. This contrast is particularly notable in how the materials respond to laser light. Specifically, road markings are characterized by their ability to reflect the laser light with a higher intensity. This difference in reflectivity is a key factor that these methods utilize to identify and analyse road markings. However, numerous factors influence the reflected laser light intensities like the range from the laser scanner to the target and incidence angle of the laser beam. Typically, the intensity of reflected laser light decreases as incident angles and ranges increase. This leads to road markings that are more distant from the scanner appearing less bright than those closer to it. To address the impact of these factors on the intensity values, we compare two methods: i) the use of gamma correction and intensity thresholding algorithms, and ii) the algorithm derived from the work of (Ye et al., 2022). Both approaches implement a distinct threshold value for each ROI. Our data does not include colour or scan angle information, but only intensity values. Thus, both used methods are based on the exploit of the intensity attribute of the points.

In the first method, we grayscale the intensity values of each block and normalize them using a gamma correction. Gamma correction is a power-low transformation used in image processing to modify the intensity values of an image. This operation can be mathematically represented as

$$O = I^{\gamma}, \tag{1}$$

where O, is the output intensity, I, is the input intensity and γ, is the gamma value. By adjusting the gamma value, which controls the relationship between pixel values and brightness, the image contrast can be enhanced. Next step in this approach is to threshold the transformed intensity values to find the high-intensity points. For this reason, we implement a multi-thresholding algorithm that uses Otsu (Otsu, 1979), Yen (Yen et al., 1995), and Li (Li and Lee, 1993) threshold methods. Each of these methods employs unique algorithms to automatically determine the optimal threshold value, for segmenting an image into foreground and background, thereby facilitating the road marking extraction. Otsu's method computes the threshold by minimizing the intra-class variance, or equivalently, by maximizing the inter-class variance of the black and white pixels. Yen's method takes a different approach by utilizing the maximum correlation criterion to determine the optimal threshold. Li's method introduces an iterative technique that seeks to minimize the cross-entropy between the original and the thresholded image. Finally, we use the statistical outlier removal (SOR) filter to mitigate the influence of noise points. The SOR filter operates on the principle of statistical analysis within a localized neighbourhood of each data point. For each point in the dataset, the filter calculates the mean distance, μ, from it to its neighbours and the standard deviation, σ, of these distances. A point is considered an outlier if the distance to its neighbours falls outside a specified range, typically defined as $\mu \pm k\sigma$, where k, is a user-defined parameter that determines the sensitivity of the filter.

The second method is derived from the work of (Ye et al., 2022) and first it utilizes a global intensity filter, which identifies road markings based on intensity information. The criteria for detecting markings are defined as:

$$\forall\, pi: \begin{cases} Road\ marking\ candidates, & if\ (I_{min} \leq I_i \leq I_{max}) \\ non - marking\ points, & otherwise \end{cases} \tag{2}$$

where I_i is the intensity values of MLS points. I_{min} and I_{max} are the minimum and maximum intensity thresholds, respectively. If the intensity value of a point falls within the predefined range, it is then considered as a potential road marking. Similar to the previous approach, the SOR algorithm is also applied in this method to address the issue of noise that may result in inaccurately determining road marking candidates.

However, despite employing robust thresholding techniques the detected road markings still contain noise. In addition, urban road markings usually present rough or damaged shapes due to vehicular traffic, weather conditions or environmental factors.

3.3 Data clustering

Since the extracted road marking points are spread out and not organized, it is essential to group them into distinct clusters before implementing the classification process. This clustering step is crucial for our analysis, which is entirely designed to operate directly with point cloud data. Unlike some methodologies, our approach avoids the intermediate step of

This contribution has been peer-reviewed. The double-blind peer-review was conducted on the basis of the full paper.
https://doi.org/10.5194/isprs-annals-X-4-W5-2024-281-2024 | © Author(s) 2024. CC BY 4.0 License.

transforming point clouds into images, maintaining the integrity of the original point cloud data.

HDBSCAN, short for *Hierarchical Density-Based Spatial Clustering of Applications with Noise*, is an advanced clustering algorithm that builds upon the concepts introduced by DBSCAN (*Density-Based Spatial Clustering of Applications with Noise).* Unlike DBSCAN, which requires the user to set a fixed distance parameter (*epsilon*) and a minimum number of points to define a cluster, HDBSCAN is more flexible. It automatically finds clusters of varying densities and eliminates the need to specify the exact number of clusters beforehand. In our analysis we prefer HDBSCAN over DBSCAN due to its advanced capabilities and flexibility. This algorithm can effectively identify clusters within data that have varying densities. This is useful when working with complex point cloud data, where road markings can vary significantly in density. Moreover, HDBSCAN requires fewer parameters to be set by the user, making it easier to use and less sensitive to parameter choice.

3.4 Road marking classification

The concept of object descriptor plays a fundamental role in the classification of objects in computer vision, serving as a foundation for identifying and categorizing objects. An object descriptor is essentially a representation of an object's key characteristics or features, such as edges, textures, shapes, or colour histograms. These descriptors capture essential information about the object's appearance and are used to differentiate one object from another. In the context of classification, these descriptors enable algorithms to recognize and categorize objects by comparing their features to those of known object classes.

In our method, for the suggested object descriptor, we consider attributes related to geometry and position. Geometry refers to the geometric characteristics of the cluster, while position refers to attributes that reflect the instance's position according to the surroundings. The structure of the object descriptor is showed in Table 1.

Sub-descriptor	Acronym	Explanation
Geometry Descriptor (GD)	*L*	Linearity
	W, l	Width, length
Position Descriptor (PD)	*curbdist*	maximum distance to the curbs
	mindist	closest perpendicular distance of the clusters' centroids
	o	cluster orientation

Table 1: The structure of the proposed object descriptor.

In the sub-descriptor of geometry, we encode 1) the attribute of linearity (L), as it helps us to classify the road markings as linear or non-linear, through Principal Component Analysis (PCA). The linear markings we detect are the road centrelines, the edge lines (lines at the road boundaries), and the zebra crossing lines. 2) the width (W) and length (l) metrics, as they serve as a constraint to determine certain types of road markings according to the standard regulations of road marking dimensions in Spain (Ministerio de Obras Públicas y Urbanismo, 1987). These attributes are measured directly from the geometric boundaries of each object. First, we apply a linear regression to fit a line that represents the direction of each cluster. After, by using PCA we align each linear cluster along its principal axes, and then we calculate the spread along these axes to find the dimensions.

In the sub-descriptor of position, we compute 1) the minimum perpendicular distance of the centroid of each cluster to the rest of the clusters (*mindist*), computed as the minimum distance of the cluster's centroid to its nearest neighbours clusters, 2) the maximum distance to the curbs (*curbdist*) measured perpendicularly from the centroid of the object to the road centreline and to both sides, and 3) the orientation (o) of the cluster according to the road direction, which is measured as the angle difference of the cluster vector and the road direction vector.

3.5 Space distribution

In our method, we start by classifying certain road markings based on their feature analysis and comparison with the object descriptor. Our aim is to distribute the space into semantically meaningful patches. For this purpose, we start by detecting zebra crossings from their centrelines as in (Treccani et al., 2022). For this reason, the OSM data for the road centrelines is used. There are 3 types of road crossings, named X crossing, T crossing, usually close to 90 degrees, and L crossing (Figure 3).

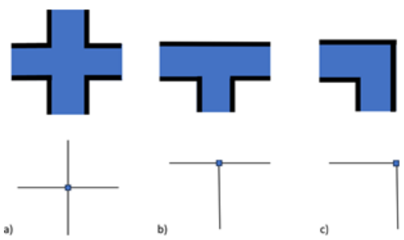

Figure 3. Types of road crossings: a) X-shape, b) T-shape, and c) L-shape.

First, we detect the crossings based on intersecting road polylines. We define the type of each crossing according to the number of connected road centrelines. By their definition, crossings refer to points where two or more road or pathways meet within an urban or rural framework. Thus, a crossing of L type, T type, or X type is defined when 2, 3, or 4 roads intersect, respectively. Having identified the intersections, it is possible to ascertain the presence of zebra crossings in the vicinity. From the classification step we already know the positions of the zebra crossings, thus we delineate the bounding boxes by generating polygons that encompass them (Figure 4).

The subsequent phase of the space distribution involves calculating the road width by utilising the curbs point cloud. The width is computed by determining the perpendicular distance from the road centreline to the nearest curb point. Finally, the width of the road at several points is known, and the number of carriageways or the existence of parking spaces is estimated. Regarding the identification of parking spaces, the shape of the curb points and the classified edge markings serve to delineate their boundaries. The road point cloud is initially separated along its centreline to facilitate the processing of each curb side. Subsequently, two lines are fitted in each side of the road, one for each curb and another for the edge markings that were identified in the preceding step. In each side, a polygon is created from the road centreline to the fitted line of the curb. Consequently, these polygons are divided along the lines of the fitted edge markings. The width of the resulting polygons determines the existence of parking spaces and the number of carriage lanes.

https://doi.org/10.5194/isprs-annals-X-4-W5-2024-281-2024 | © Author(s) 2024. CC BY 4.0 License.

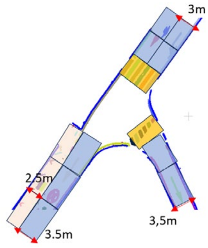

Figure 4. Space distribution from a theoretical point of view.

4. Experiments and results

4.1 Case study

The method was applied and evaluated in a 2-kilometer urban street network located in (González-Collazo et al., 2024). Point clouds were captured using a combination of handheld and car-mounted Mobile Laser Scanners to maximize data completeness. Point clouds were submitted to a semi-automated labelling process supported by heuristic and Deep Learning tools, resulting in eight specific classes: *road, sidewalk, curb, buildings, vehicles, vegetation, poles, and others.* For this work, just *road*, and *curb* classes were used. Figure 5 shows a partial view of the input dataset.

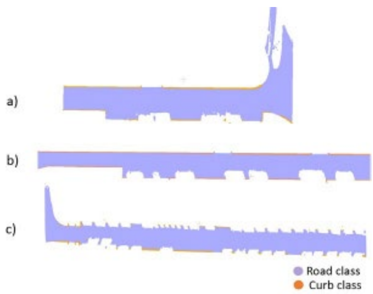

Figure 5. Classified data of a) street segment D, b) street segment H, and c) street segment I of our input point cloud.

It is important to highlight that the point cloud lacks RGB information, but it includes LiDAR intensity. Further information about the point cloud segmentation can be found in (González-Collazo et al., 2024).

4.2 Pre-processing

The dataset consists of eleven segments of five urban roads, with each segment extending about 200 m. The radius, r, parameter we used for the cylindrical ROI generation had a value of 5. After the pre-processing phase we obtained in total 69 ROIs, each one with a length of 20 m, for all the streets. Table 2 summarizes number of ROIs per street, as well as the number of points per ROI.

Street	Segment	Number of ROIs	Number of points/Segment
Frei Rosendo Salvado	L	3	2,411,709
	K	7	4,977,534
	G	3	1,845,508
Pedro de Mezonzo	H	11	6,379,656
	I	6	4,008,889
	J	6	3,456,851
Ramón Cabanillas	F	8	3,766,380
Fernando III o Santo	E	8	4,014,996
	D	7	3,017,696
Santiago de Chile	M	5	4,949,471
	N	6	5,868,652

Table 2: Main characteristics of the street segments.

4.3 Intensity analysis

We validated our automated road marking extraction results from both methods by computing the accuracy, precision, recall and F1 score metrics (Ye et al., 2022).

Metric results		
Metric	Gamma correction and intensity thresholding algorithms	Method from (C. Ye et al., 2022)
Accuracy	0.96	0.96
Precision	0.84	0.85
Recall	0.53	0.55
F1	0.62	0.64

Table 3: Metric results for intensity thresholding evaluation.

Table 3 shows the results of the metrics described above, which indicate a preference for the method derived from (Ye et al., 2022). Their approach edges forward with a higher precision of 0.85, recall of 0.55, and an F1 score of 0.64. The higher recall and F1 score suggest an improved balance between sensitivity and precision, marking its efficiency in identifying true positives while maintaining a lower rate of false positives. Thus, we proceeded with the method of (Ye et al., 2022), due to its superior performance in precision and recall, as shown by the comparative metrics.

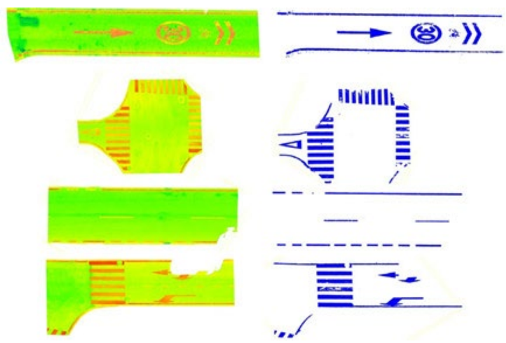

Figure 6. Road marking detection after the intensity analysis algorithm.

The behaviour of our algorithm in the predictions was as expected. The best identified road markings were the ones with higher number of points (arrows, triangles) than the ones with less (dashed lines). Thus, the road segments that consist of big markings gave higher rates than the ones that contain small markings. Furthermore, some of the markings were not detected because of lower intensity values of the laser return from them (Figure 7).

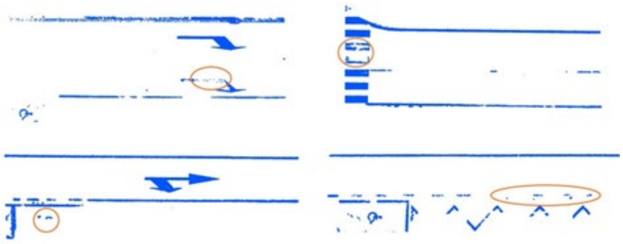

Figure 7. Undetected parts of road markings.

4.4 Data clustering

In our analysis, the implementation of the HDBSCAN algorithm showed significant efficiency in clustering most of the extracted road marking points from the point cloud data. The parameter used is the minimum cluster size and it determines the smallest size a group of points must have to be considered a valid cluster. For our study, we chose a value of 10 for this parameter. This decision was based on the typical size and density of road markings in our point cloud data, where clusters smaller than this threshold often corresponded to noise or irrelevant features rather than actual road markings.

As shown in Figure 8, the proposed method successfully clustered the road marking point clouds into isolated meaningful objects. Each colour represents a distinct road marking cluster.

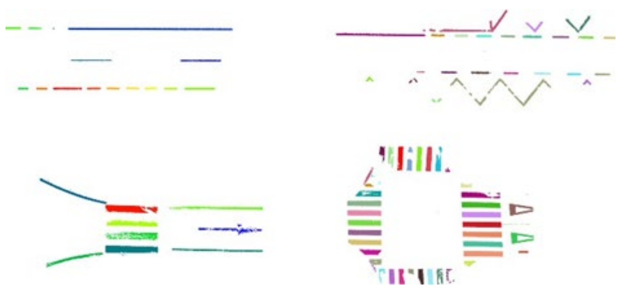

Figure 8. Road marking clusters.

However, instances of erroneous segmentation are observed in some cases. These inaccuracies appear when points are incorrectly grouped together or when actual objects are divided into multiple segments. Such segmentation errors can arise from various factors, including noise within the point cloud data, similar features between distinct objects, varying point density, or occlusions and shadows that obscure parts of the objects.

4.5 Road marking classification

Once the locations of the crossings have been identified, it can be reasonably assumed that zebra crossings will be found in proximity. A buffer zone of 14 m was therefore defined around the node to ascertain the presence of any clusters with a shape like that of zebra crossings. Clusters with a linearity value higher than 0.95 were classified as lines and were distinguished from the remaining markings. According to Spanish regulations, zebra crossings must be between 0.5 m and 0.7 m wide and less than 5 m long. Consequently, clusters that did not comply with these regulations were excluded from further analysis. It is also known that the zebra stripes must be separated by a certain distance in accordance with the regulations. Accordingly, the minimum perpendicular distance between the centroids of the clusters was set to 1 m. Following the filtering process, the zebra crossings of our intersections were identified. Finally, the HDBSCAN algorithm was applied to cluster each stripe to the correct zebra crossing (Figure 9a).

The remaining linear markings were classified according to a width threshold between 0.1 m and 0.2 m, which represents the limits of the width dimension of the edge and centre lines in accordance with the regulations. Second, these markings are parallel to the road direction. Consequently, an angle threshold of 10 degrees was set, below which clusters are parallel to the road. Conversely, clusters with an angle greater than 170 degrees (which is also considered to be parallel) were retained. Finally, the edge lines and the centre lines were distinguished based on their distance from the curbs. For a cluster to be considered a border line, the maximum distance from the curbs must be less than 3 m. Figure 9b shows some of the markings classified as edge lines. The application of the described object descriptor has yielded significant results in the classification of five zebra crossings, as well as linear markings located at the borders of the roads and of centre line markings from our point cloud data.

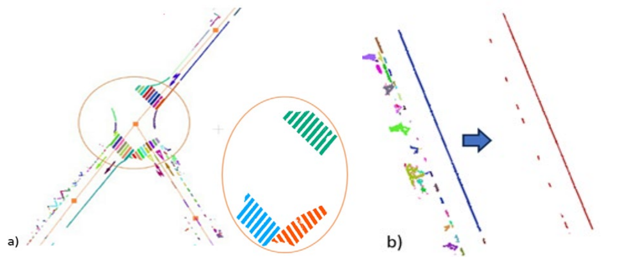

Figure 9. Road marking classification of a) zebra crossings, b) edge markings.

4.6 Space distribution

Two T-type crossings have been identified in our case study, as illustrated in Figure 10. In the vicinity of these two intersections, five zebra crossings have been identified and classified, and in each one of them a bounding box was delineated, indicating the space reserved for pedestrians. According to the Spanish regulations for roads the width of each carriage line in urban roads is between 3 m and 3.5 m. Thus, we concluded that if the road width is higher than 6 m, there are more than 1 carriage lines and if is less than 6 m we detected only 1 carriage line. Also, the standard width for parking lane is between 1.8 m and 2.5 m, so in the areas that the road width is 3.5 m < Road width ≤ 6 m, arises the conclusion that 1 carriage line and parking only from one side of the road exist. Moreover, in cases that the parking width was approximately 8.5 m we detected 1 carriage line and parking from both sides of the road, and if it was higher than 8.5 m but lower than 9 m, 2 carriage lines and parking space only from one side were identified. Finally, in our case study there were a few streets with road width higher than 9 m. In these cases, we concluded that 2 carriage lines and parking spaces for both sides of the road exist. According to the above dimensions and considering the presence of the curbs we delineated the bounding boxes for 3 different functional spaces in the urban area: parking space, zebra crossing space and road carriage line space respectively. Figure 11 displays the enclosed rectangles that surround the zebra crossing markings, as well as the bounding boxes for a carriage line and a parking space that are generated from our method.

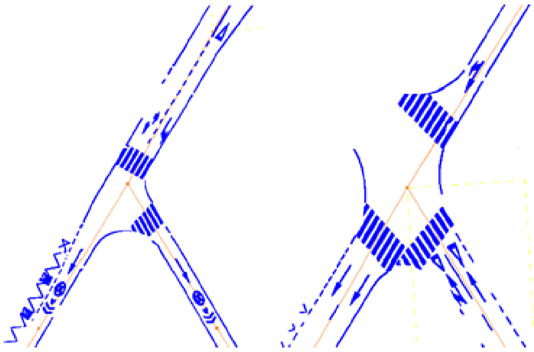

Figure 10. Crossing detection.

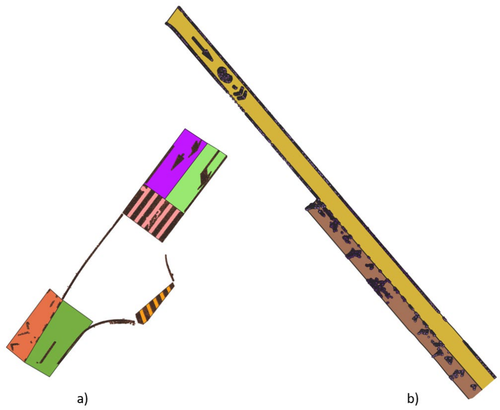

Figure 11. Road space distribution in bounding boxes. a) zebra crossings, b) carriage lane and parking space.

5. Conclusions

This paper presents a comprehensive method to automatically detect road markings from point cloud data based only on the intensity attribute of it, demonstrating an initial approach on the conceptual distribution of the road space and semantically enrichment from the road marking extraction.

The starting point of our work was the road and curb class from a semantically segmented point cloud. The pre-processing section of this study prepared the road class point cloud data for subsequent analysis. By addressing the massive volume and intensity inconsistencies within the data, this phase set the basis for more accurate and efficient road marking extraction. The refinement of ROIs, especially in addressing the challenges caused by curved roads, showed the adaptability and precision of our methodology.

By employing intensity-based analysis, our method effectively addresses the variability inherent in point cloud data, resulting from environmental factors and scanning inconsistencies. The use of advanced clustering algorithms such as HDBSCAN marked a significant advancement in grouping extracted road marking points. The development of an object descriptor for road marking classification that incorporates both geometric and positional attributes of clusters, differentiated between linear and non-linear road markings and the identification of zebra crossings based on their width, length, and parallelism. This classification scheme is an integral part of the semantic enrichment of the urban space and provides a detailed understanding of certain functions of road markings within the urban landscape.

The main contribution of our methodology extends into the critical aspect of space distribution, which is integral to understanding urban functionality. Through the analysis of road markings, including their geometry and relative positioning, we have been able to segment urban spaces into functionally distinct areas. Moreover, the ability to distinguish between different types of crossings and to accurately measure road and lane widths has provided a view of urban traffic flow and pedestrian movement patterns.

In this study, we have primarily used heuristic methods for the analysis of the road markings, demonstrating considerable success in interpreting urban road environments. Looking ahead, exploring machine learning tools to further refine the classification of road markings is a promising area for future research. Additionally, future work will aim to expand the scope of our spatial distribution analysis beyond the flat plane of the road surface to include a three-dimensional perspective, extending also to encompass sidewalks. This expansion will enable a more complete representation of urban spaces, capturing the complexity of the urban environment in greater detail. Eventually, the goal is to achieve a comprehensive mapping of urban spaces into connected 3D boundaries, each semantically enriched to provide a deep understanding of their function and significance within the urban network. This future direction promises to significantly advance our ability to digitally represent and navigate urban environments, providing valuable insights for urban planning, autonomous navigation, and the creation of smart cities.

Acknowledgements

This work was partially supported by human resources grant RYC2020-029193-I funded by MCIN/AEI/10.13039/501100011033 and FSE 'El FSE invierte en tu futuro', by grant ED431F 2022/08 funded by Xunta de Galicia, Spain-GAIN, and by the projects PID2021-123475OA-I00 funded by MCIN/ AEI /10.13039/501100011033/ and by FEDER 'Una manera de hacer Europa' and CNS2022-135730 funded by MCIN/AEI /10.13039/501100011033 and by European Union NextGenerationEU/PRTR. The statements made herein are solely the responsibility of the authors.

References

Babić, Dario, Fiolic, M., Babić, Darko, Gates, T., 2020: Road Markings and Their Impact on Driver Behaviour and Road Safety: A Systematic Review of Current Findings. *J Adv Transp,* 1–19. doi.org/10.1155/2020/7843743

Barçon, E., Landes, T., Grussenmeyer, P., Berson, G., 2022: Extraction of road markings from mls data: a review. *Int. Arch. Photogramm. Remote Sens. Spatial Inf. Sci.*, XLVIII-2/W1, 7–14. doi.org/10.5194/isprs-archives-XLVIII-2-W1-2022-7-2022

Certad, N., Morales-Alvarez, W., Olaverri-Monreal, C., 2022: Road Markings Segmentation from LIDAR Point Clouds using Reflectivity Information. *2022 IEEE International Conference on Vehicular Electronics and Safety (ICVES), Bogota, Colombia,* 1–6. doi.org/10.48550/arXiv.2211.01105

Cheng, Y.T., Patel, A., Wen, C., Bullock, D., Habib, A., 2020: Intensity Thresholding and Deep Learning Based Lane Marking Extraction and Lane Width Estimation from Mobile Light Detection and Ranging (LiDAR) Point Clouds. *Remote Sens*, 12. doi.org/10.3390/RS12091379

Diakité, A.A., Zlatanova, S., 2018: Spatial subdivision of complex indoor environments for 3D indoor navigation. *International Journal of Geographical Information Science*, 32, 213–235. doi.org/10.1080/13658816.2017.1376066

Fang, L., Sun, T., Wang, S., Fan, H., Li, J., 2022: A graph attention network for road marking classification from mobile LiDAR point clouds. *International Journal of Applied Earth Observation and Geoinformation*, 108. doi.org/10.1016/j.jag.2022.102735

Golakiya, H.D., Patkar, M., Dhamaniya, A., 2019: Impact of Midblock Pedestrian Crossing on Speed Characteristics and Capacity of Urban Arterials. *Arab J Sci Eng*, 44, 8675–8689. doi.org/10.1007/s13369-019-03786-x

González-Collazo, S.M., Balado, J., Garrido, I., Grandío, J., Rashdi, R., Tsiranidou, E., Del Río-Barral, P., Rúa, E., Puente, I., Lorenzo, H., 2024: Santiago Urban Dataset SUD: Combination of Handled and Mobile Laser Scanning point clouds. *Expert Syst Appl*, 238B. doi.org/10.1016/j.eswa.2023.121842

González-Collazo, S.M., Balado, J., González, E., Lorenzo, H., Díaz-Vilariño, L., 2022: Defining the Functional Space of Bus Stops from MLS Point Clouds. *ISPRS Ann. Photogramm. Remote Sens. Spatial Inf. Sci*., X-4/W2, 77–82. doi.org/10.5194/isprs-annals-X-4-W2-2022-77-2022

Hoang, T.M., Nam, S.H., Park, K.R., 2019: Enhanced detection and recognition of road markings based on adaptive region of interest and deep learning. *IEEE Access*, 7, 109817–109832. doi.org/10.1109/ACCESS.2019.2933598

Li, C.H., Lee, C.K., 1993: Minimum cross entropy thresholding. *Pattern Recognit*, 26, 617–625. doi.org/10.1016/0031-3203(93)90115-D

Ma, L., Li, Y., Li, J., Wang, C., Wang, R., Chapman, M.A., 2018: Mobile laser scanned point-clouds for road object detection and extraction: A review. *Remote Sensing*, 10. doi.org/10.3390/rs10101531

Meghjani, M., Luo, Y., Ho, Q.H., Cai, P., Verma, S., Rus, D., Hsu, D., 2019: Context and Intention Aware Planning for Urban Driving. *IEEE/RSJ International Conference on Intelligent Robots and Systems (IROS),* 2891–2898. doi.org/10.1109/IROS40897.2019.8967873

Mi, X., Yang, B., Dong, Z., Liu, C., Zong, Z., Yuan, Z., 2021: A two-stage approach for road marking extraction and modeling using MLS point clouds. *ISPRS Journal of Photogrammetry and Remote Sensing*, 180, 255–268. doi.org/10.1016/j.isprsjprs.2021.07.012

Ministerio de Obras Públicas y Urbanismo, 1987: *Norma de carreteras 8.3-IC. Señalización de Obras.*

Nikoohemat, S., Diakité, A., Zlatanova, S., Vosselman, G., 2019: Indoor 3D modelling and flexible space subdivision from point clouds. *ISPRS Ann. Photogramm. Remote Sens. Spatial Inf. Sci.*, IV-2/W5, 285–292. doi.org/10.5194/isprs-annals-IV-2-W5-285-2019

Otsu, N., 1979: A Threshold Selection Method from Gray-Level Histograms. *IEEE Trans Syst Man Cybern*, 9, 62–66. doi.org/10.1109/TSMC.1979.4310076

Rasouli, A., Tsotsos, J.K., 2018: Joint Attention in Driver-Pedestrian Interaction: from Theory to Practice. doi.org/10.48550/arXiv.1802.02522

Treccani, D., Díaz-Vilariño, L., Adami, A., 2022: Accessible path finding for historic urban environments: feature extraction and vectorization from point clouds. *Int. Arch. Photogramm. Remote Sens. Spatial Inf. Sci.*, XLVI-2/W1, 497–504. doi.org/10.5194/isprs-archives-XLVI-2-W1-2022-497-2022

Wen, C., Sun, X., Li, J., Wang, C., Guo, Y., Habib, A., 2019: A deep learning framework for road marking extraction, classification and completion from mobile laser scanning point clouds. *ISPRS Journal of Photogrammetry and Remote Sensing*, 147, 178–192. doi.org/10.1016/j.isprsjprs.2018.10.007

Yang, R., Li, Q., Tan, J., Li, S., Chen, X., 2020: Accurate Road Marking Detection from Noisy Point Clouds Acquired by Low-Cost Mobile LiDAR Systems. *ISPRS Int. J. Geo-Inf*., 9. doi.org/10.3390/ijgi9100608

Yang, Y., Li, M., Ma, X., 2020: A Point Cloud Simplification Method Based on Modified Fuzzy C-Means Clustering Algorithm with Feature Information Reserved. *Math Probl Eng*. doi.org/10.1155/2020/5713137

Ye, C., Zhao, H., Ma, L., Jiang, H., Li, H., Wang, R., Chapman, M.A., Junior, J.M., Li, J., 2022: Robust Lane Extraction from MLS Point Clouds Towards HD Maps Especially in Curve Road. *IEEE Transactions on Intelligent Transportation Systems*, 23, 1505–1518. doi.org/10.1109/TITS.2020.3028033

Ye, X.Y., Hong, D.S., Chen, H.H., Hsiao, P.Y., Fu, L.C., 2020: A two-stage real-time YOLOv2-based road marking detector with lightweight spatial transformation-invariant classification. Image. *Vis Comput,* 102. doi.org/10.1016/j.imavis.2020.103978

Yen, J.C., Chang, F.J., Chang, S., 1995: A new criterion for automatic multilevel thresholding. *IEEE Transactions on Image Processing*, 4, 370–378. doi.org/10.1109/83.366472